Key considerations in infrared simulations of the missile-aircraft engagement

Maria S. Willers[a] and Cornelius J. Willers[b]

[a] Denel Dynamics, P.O. Box 7412, 0046 Centurion, South Africa
[b] CSIR, P.O. Box 395, 0001 Pretoria, South Africa

ABSTRACT

The development of modern imaging and non-imaging infrared missile signal processing and countermeasure techniques strongly relies on high quality simulated imagery of target and countermeasure signatures. Likewise, the development of an effective countermeasure technique or system for aircraft self-protection requires accurate missile behaviour modelling. The development of these algorithms and protocols can be done most effectively in an accurate infrared imaging simulation. This paper investigates the requirements for such a simulation system, supporting the evaluation of the missile behaviour in the missile-aircraft engagement scenario.

The development and evaluation of target detection and tracking algorithms, or countermeasure systems, requires a comprehensive simulation environment where thousands of missile flights can be simulated, covering a wide variety of scenarios and signature conditions. The missile seeker algorithms generally detect and classify targets based on intensity, spatial and dynamic characteristics.

The key considerations identified for such an imaging infrared simulation system are: 1) radiometric accuracy in all spectral bands, i.e. sunlight and thermal radiance to provide correct colour ratios; 2) accurate emitting source surface temperature behaviour, be it by aerodynamic or thermodynamic heating; 3) high fidelity geometrical and spatial texture modelling to provide shape of targets and countermeasures; 4) true dynamics and kinematic behaviour in six degrees of freedom; 5) detailed modelling of signatures and backgrounds; 6) accurate atmospheric transmittance and path radiance models; 7) realistic rendering of the scene image in radiometric, spatial and temporal terms; and 8) comprehensive sensor modelling to account for primary and second order imaging effects.

This paper briefly analyses the broader framework of requirements for an imaging simulation system, in the 0.4 to 14 μm spectral bands. An existing imaging simulation system, OSSIM, is used to evaluate the identified key requirements for accurately simulating the missile-aircraft engagement scenario. Parameters considered include signature spectral colour ratio, spatial shape, kinematics, temporal behaviour, as well as the effect of the atmosphere and background. From this analysis the significance and relevance of the modelled signature elements are reviewed, thereby confirming the key requirements for simulating the missile-aircraft engagement.

Keywords: infrared simulation, missile-aircraft engagement, signature elements, image rendering

1. INTRODUCTION

The development of modern imaging and non-imaging infrared missile signal processing and countermeasure techniques strongly relies on high quality simulated imagery of target and countermeasure signatures. Likewise, the development of an effective countermeasure technique or system for aircraft self-protection requires accurate missile behaviour modelling. The development of these algorithms and protocols can be done most effectively in an accurate infrared imaging simulation.

This paper investigates the requirements for such a simulation system, supporting the evaluation of the missile behaviour in the missile-aircraft engagement scenario.

Further author information: (Send correspondence to M.S.W.)
M.S.W.: E-mail: riana.willers@deneldynamics.co.za, Telephone: +27-12-671-1901
C.J.W.: E-mail: nwillers@csir.co.za, Telephone: +27-12-841-4261

Technologies for Optical Countermeasures IX, edited by David H. Titterton, Mark A. Richardson,
Proc. of SPIE Vol. 8543, 85430N · © 2012 SPIE · CCC code: 0277-786/12/$18 · doi: 10.1117/12.974801

The missile-aircraft engagement demonstrates complex interactions between the aircraft and missile in particular, but affected by environmental effects. These interactions typically play out in an iterative cycle of action and reaction between the two major players. Section 2 further investigates the dynamics of the engagement process.

As the sophistication of weapons and countermeasures grow, the parameters and features used in these measures increase in number and sophistication. Each generation of missile or countermeasure attempts to outdo the adversary and in the process, adds new complexity to the interaction.[1] As can be expected, any simulation of such engagements must keep up with the details of the hardware systems.

Missile performance depends on many factors, affecting the seeker, tracking and guidance behaviour. We investigate the requirements for the modelling and simulation of significant signature elements, i.e. which elements are key to an accurate missile-aircraft engagement simulation? This review focusses on the physics and seeker sensor and algorithm driven requirements, but also considers other factors affecting these key elements.

The identified key requirements are tested in a well proven, working simulation system. In the interest of brevity, some requirements are investigated in detail, while others are only briefly considered—this should not be taken as prioritisation. Emphasis is placed on the importance of accurate in-band spectral modelling and its application in colour ratios. Colour ratio is as important in suppressing sunlit background (i.e. clouds) as in suppressing countermeasure flares.

2. THE MISSILE-AIRCRAFT ENGAGEMENT

2.1 The engagement in context

According to Kopp[2] "A typical missile engagement requires that the aircraft be detected, tracked, its flight path predicted, and missiles launched and guided to impact for the engagement to be successful. Should any of these phases of the engagement be disrupted or defeated successfully, the engagement will not be successful."

First generation infrared (IR) missiles homed in on the heat produced by the hot exhaust pipe of the aircraft. The attacking aircraft had to manoeuvre to a position behind its target before it could fire the IR missile. These missiles were only effective at close range, could be distracted by other hot sources (e.g. the sun or back-lit clouds) and did not have head-on attack capability. The introduction of IR missiles triggered the development of countermeasure techniques to defeat these weapons, thereby protecting the aircraft. Missile countermeasures such as on-board jamming systems and Magnesium, Teflon and Viton (MTV) flares became an integral part of the missile-aircraft engagement. As stated by Titterton,[1] "this was the beginning of a classic 'cat and mouse' activity between the measures and the countermeasure, which continues to this day."

In response to the introduction of countermeasures, missile manufacturers attempted to swing the missile-aircraft engagement in their favour by developing counter-countermeasures (CCMs) in the IR seekers to negate the effect of the flares.[3] Counter-countermeasure techniques can be implemented in hardware, or in the missile software algorithms. The *rise rate trigger* senses a rapid rise of radiated flare intensity, comparing it with an acceptable rise rate for an aircraft engine power setting change. *Trajectory sensing* uses the fact that, relative to the aircraft, flares generally lag behind the aircraft (due to aerodynamic drag) and fall downwards (because of gravitational acceleration). The rate of separation between the flare and the target aircraft is also a feasible counter-countermeasure. *Spectral discrimination* is used to discriminate spectrally between the decoy and the aircraft exhaust plume, by comparing their radiances in two different wavelength bands using a two-colour detector.

CCM development in IR seekers stimulated various flare developments to improve the flare decoy's success against the missile seekers. The main areas of development being[3] (1) burn profile shaping, where the flare energy is manipulated over the burn time period to mimic typical jet profiles, (2) aerodynamic and thrusted flares designed to counter the trajectory sensing ability and separation trigger of some missiles, (3) multi-spectral flares with cooler burning materials to defeat the two-colour missile, (4) smart dispensers designed to carry flare cocktails to defeat all the different threat types, and (5) multi-shot flares which enables a combination of flare types in one payload.

Modern developments include directed energy countermeasure (DIRCM) systems, using IR sources or lasers to deceive (jam), dazzle or damage the seeker.[1] While compensating fully for physical damage is beyond the reach of missile seeker processing, seeker processing has to compensate for, or at least mitigate some of the effects of deception, dazzling and damage. Often, such compensation requires missile system-level intervention (e.g. guidance adjustments).

It is evident that it becomes more and more challenging to produce IR seekers that can effectively discriminate between the aircraft and the countermeasures. New generation CCM techniques require functionality across all major hardware components, operating in a coordinated manner to achieve the countermeasure effectiveness. Major new requirements include sensors that provide images of the target scene and image processing algorithms extracting detailed information from these images. Some missile seekers employ single colour sensors, while others use two-colour sensors.

The emergence of the new seeker technologies demands powerful development environments capable of handling the complexities of the imaging seekers. Image processing algorithm development requires a development process of endlessly repeated experiments, training and testing. A computer-based simulation environment is essential in this process.

2.2 Review of the engagement

The engagement process is a dynamic process (shown in Figure 1), with periods of stable tracking (circular trajectories) and unstable intermediate periods of re-acquisition (spiral trajectories). The missile (left-hand side) and aircraft (right-hand side) are locked in a sequence of actions and reactions. After the initial missile acquisition (inner green dot) the missile tracks the aircraft in a more or less stable system (pseudo-linear behaviour). The aircraft reacts to the engagement by some action, e.g. a countermeasure deployment (inner yellow star), which may result in loss of lock (spiral trajectory). The missile reacts by re-acquiring the aircraft, as the iterative process continues. Along the outward trajectories the stakes for both the missile and aircraft grow rapidly and the risk of failure on both sides explodes. The growth in risk stems from the increased complexity of the engagements—complexity arising from hardware sophistication, but also from the cumulative effects of subsequent disturbances in the engagement.

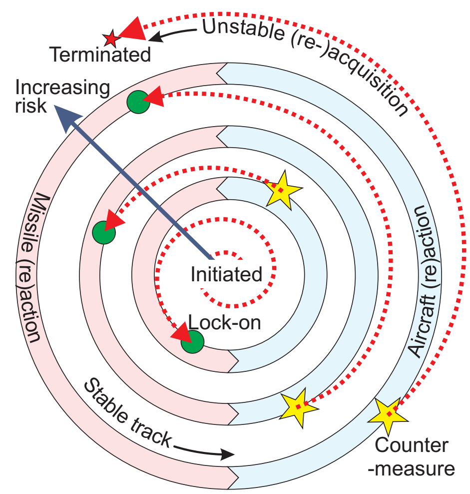

Figure 1: The missile-aircraft engagement.

The critical acquisition and loss-of-lock events are highly non-linear events. During these events, a trivially small perturbation in the unfolding chain-of-errors and chain-of-successes will hugely affect the outcome of the events. It should be self-evident that if the hardware interaction is so sensitive to small perturbations, the simulation of the engagement should be even more sensitive. It is essential therefore, that the simulation gives attention to the smallest of details. Some of these details are investigated in Section 6.

The tactical missile system used against aircraft includes several subsystems: airframe, flight control, fuze, propulsion, telemetry, data link, warhead and seeker.[4] The seeker of an imaging IR missile provides steering commands to the flight control system to intercept the target aircraft. The seeker comprises (1) the dome to protect the seeker from aerodynamic forces and the weather; (2) an optical system to focus the incident scene flux onto the detector; (3) a stabilised gimbal system to point the optical path towards the identified target and to minimise jitter in the image; (4) an IR detector to collect the flux and generate an image; and (5) an image processor to analyse the image and to provide tracking errors to the tracking loop for missile guidance. An analysis of the missile-aircraft engagement, focussing on the seeker functionality is shown in Figure 2. IR missile seeker sensor and image processing requirements are discussed in the next section.

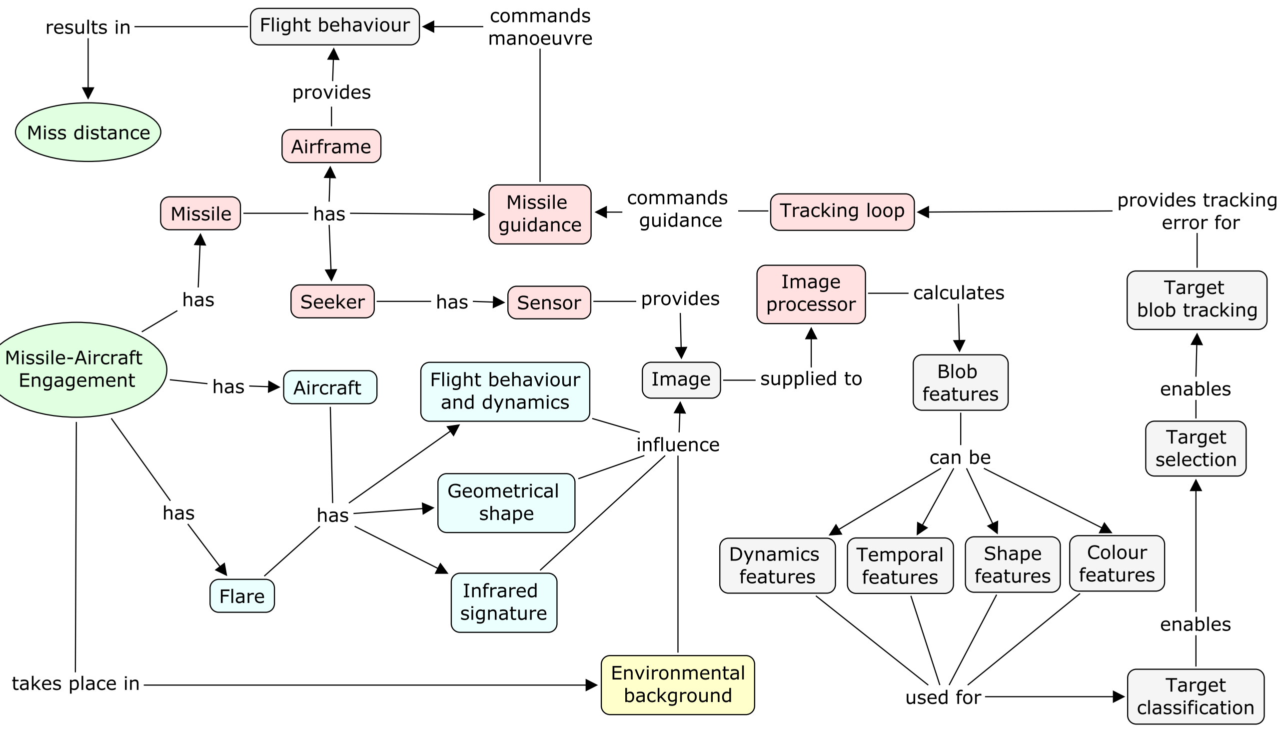

Figure 2: The missile-aircraft engagement, emphasising missile seeker functions.

3. IMAGING MISSILE SEEKER REQUIREMENTS

3.1 Seeker sensor requirements

Modern seeker sensors provide single or two-colour images with image sizes ranging from small (128×128) in air-intercept seekers to relatively large (384×288) or even larger in air-to-ground seekers. Image frame rates range from 50 Hz to 200 Hz, but higher frame rates pose a significant challenge to subsequent image processing. Spectral bands range from near IR (visible to 2.5 μm) and middle IR (3–5 μm) for air-intercept seekers and long wave (8–12 μm) for air-to-ground missiles. Images are formed by staring arrays or scanning linear vectors sweeping across the sensor's field of view.

Missile seeker sensors are subject to particularly difficult challenges, such as (1) very wide dynamic range scene requirements (hot flares to aircraft fuselages), (2) large shifts in operating point due to dome heating and internal operating temperature (stressing detector non-uniformity and narcissus corrections), (3) rapid scene variations playing havoc with operating points and gain settings, and (4) extreme sensitivity requirements to detect faint targets at long range.

A simple calculation shows that the 3–5 μm radiance ratio of an MTV flare to an aircraft fuselage in the same image to require 15 bits signal dynamic range. The intensity of a point source target decreases by a factor of $\frac{1}{R^2}$, where R is the distance separating the heat source from the sensor—an equivalent of a further 5-bits of dynamic range, as the target moves from 2 km to 10 km. Hence, the total signal variation from a faint long distance aircraft to a close range flare signature requires approximately 20-bits total sensor dynamic range.

Scanning linear array sensors provide countermeasure hardening benefits above staring arrays,[5] but also introduce unique difficulties. A limitation of staring array sensors is the fill factor: detector elements cannot touch, leading to loss of sensitivity, while scanning linear arrays, in staggered configuration, can provide 100% coverage with larger detector elements. Non-uniformity correction is difficult in both types of sensors, but reportedly easier in linear array sensors.[5]

In the medium to longer term, multi-colour staring arrays can be expected, while current technology limits operational missiles to single colour staring arrays. Scanning linear vectors readily provide two-colour images with current technology.[6,7]

3.2 Seeker algorithm requirements

The availability of a full image of the scene makes it possible for seeker algorithms to extract much more information from a scene than did previous generations of seekers. Some seekers also provide multi-spectral images. The availability of more, and better quality information of the target scene makes it possible to use more complex features of the objects in the scene. The more sophisticated features and algorithms increase the probability of differentiating between the countermeasures and the platform they protect.

A study on the concepts associated with the processing of military data to find and recognise targets[8] confirmed the commonly known target identification process as: (1) pre-processing to suppress noise, remove trends and enhance spatial discontinuities (edge enhancement), (2) segmentation to isolate blobs, (3) feature extraction from the blobs, and (4) processing of the features for decision making (classification). The key objective in the sequence is to classify objects in the scene into targets and non-targets. If any object can be classified, its presence in the image can be handled appropriately.

In this context, classification is the processing required in order to declare a region of interest or object in the image (also known as a blob*), as belonging to one of a number of pre-defined classes. The requirement is to classify blobs as belonging to a target (i.e. aircraft), countermeasure (flare or DIRCM), cloud or other background feature (clutter). Once the blobs are classified, decisions can be made regarding tracking or rejecting particular blobs in the image.

Figure 2 indicates at least four types of features that can be employed in imaging seekers: (1) shape features (calculated from image pixel values), (2) temporal features (change of features with time), (3) dynamic features (movement of objects in the image), and (4) colour features (properties in multi-spectral images). This section will investigate each of these types of features.

Labonte and Deck[9] give a detailed list of blob **shape features** assumed to be used in imaging missile algorithms. These features include pixel intensity features (maximum, average, moments), shape features (centroid, moments of inertia, eccentricity, compactness, radial distance, etc.), and invariant features (normalised intensity, normalised average intensity, normalised moments, etc.). Target intensity depends on the atmospheric transmittance between the target object and the observer. In order to compensate the effect of the atmosphere and obtain characteristics that are proper to the observed objects themselves, features that are ratios of the intensities are considered. These features are known as invariant features and are invariant under translation and rotation in a plane perpendicular to the line of sight. Particularly useful shape intensity and spatial features for IR target identification are the ratio of the object length to its width, the standard deviation of the pixel values on the object, the maximum intensity of object pixels and the object complexity (the ratio of border pixels to total number of pixels).[10]

Temporal features consider the change of features with time, compared to some predetermined baseline. One example of a temporal feature is the intensity rise time of a blob. Flares were originally designed to reach their peak intensity very rapidly in order to effectively protect airborne targets. This inherent characteristic of the flare is exploited and used as a discrimination technique.[11] If a seeker detects a rapid change in intensity, it triggers the flare detected flag and responds appropriately. DIRCM sources can be identified likewise, provided the sensor maintains operational status.

Dynamic features evaluate the movement of objects in the image, relative to each other or in inertial space. A common dynamic feature is line of sight (LOS) rate. This technique discriminates non-propelled flares from the target based on its motion in the field of view,[11] or the movement of the indicated target blob relative to other background blobs in the field of view. The seeker processing maintains tracks of all blobs in the image and, if the LOS change exceeds a certain threshold, the blob is flagged as a non target (countermeasure or background). Discrimination by dynamic features give rise to propelled flares to lower the perceived LOS rate. The dynamic behaviour of the target is exploited in the classification process to allow for detection of targets even in very cluttered environments.[12]

Colour features (also know as spectral distribution features) describe the spectral properties of a blob in a multi-spectral image. A common use of colour features is two-colour discrimination.[11] Seekers equipped with

*A blob is a region in an image of touching pixels, or pixels in immediate proximity, with a shared or common status. All pixels in an image that belong to a blob are of foreground status. All other pixels are of background status.

dual mode detectors view a scene in two separate bands of the spectrum. The seeker compares the spectral distribution ratio of the various targets in the field of view to a predefined threshold. If a target does not meet the two-colour ratio criteria, it is classified as a flare and rejected. Colour features are less effective against laser-based countermeasures, resulting from the monochromatic nature of these sources. Later generation flares produce a signature ratio close to that of aircraft plumes and as a result are more difficult to reject.

4. SIMULATION REQUIREMENTS

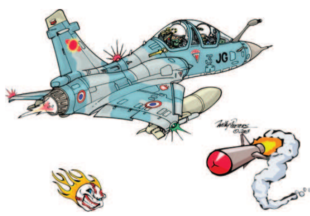

			Simulation key considerations																											
			Natural laws of physics														Image rendering					Sensor modelling								
			Radiometry					Atmosphere																						
			Spectral calculations	Thermal self-radiation	Reflected sunlight	Reflected sky radiance	Ambient radiation	Transmittance	Radiance	3D geometry & 2D texture	Thermal modelling	Temporal modelling	6-dof kinematics modelling	Aerodynamics modelling	Mechanical modelling	Control systems modelling	Anti-aliasing	Floating point calculations	Spatial resolution	Image registration	Multiple spectral bands	Optics	Dome heating	Detector properties	Detector & electronic noise	Scanning effects	Temporal temperature effects	Signal transfer function	Time delays	Simulation infrastructure
Real world requirements	Aircraft	Geometry								x																				x
		IR signature	x	x	x	x	x	x	x		x	x																		x
		Flight & dynamics											x	x																x
	Flare	Geometry								x																				x
		IR signature	x	x			x	x	x		x	x																		x
		Flight & dynamics											x	x																x
	Background	Sky	x	x	x				x		x																			x
		Sun	x	x				x		x	x	x	x																	x
		Clouds	x	x	x	x	x	x	x	x	x	x																		x
		Terrain & sea	x	x	x	x	x	x	x	x	x	x																		x
	Missile	Airframe flight behaviour										x	x	x	x	x														x
		Guidance										x	x			x														x
		Seeker: Sensor	x								x	x			x	x	x	x	x	x	x	x	x	x	x	x	x	x	x	x
		Seeker: Image processor																												x
		Seeker: Gimbal & tracking loop										x	x		x	x														x

Figure 3: Simulation key considerations required by the real world (pictures[13]).

The missile-aircraft engagement plays off in the real world where four key elements dictate the requirements for simulation: (1) the aircraft, (2) the flare, (3) the environmental background and (4) the missile. These elements are weapon and application specific. Analyses of the missile-aircraft engagement diagram in Figure 2 and the seeker requirements discussed in the previous section, identify the key considerations for imaging simulation as summarised in Figure 3. The relevant simulation key considerations for each real world element are indicated in Figure 3 and will be discussed in this section.

The *aircraft, flare* and *background* form part of this scene and influence the appearance of blobs in the missile seeker sensor image. To satisfy the requirements on the blob features as depicted in Figure 2, the geometrical shape, infrared signature and flight behaviour and dynamics of the target and flare must be described by the **natural laws of physics** in the areas of (1) radiometry, (2) radiative transfer through mediums (atmosphere), (3) geometrical and texture description, (4) thermal properties, (5) temporal behaviour, (6) six degrees of freedom (6-dof) kinematics and (7) aerodynamics.

Target identification against clutter is one of the main challenges of the missile target detection algorithm developer. The clear sky, sun, clouds, terrain and sea define the background clutter in missile seeker images and must be modelled in terms of the natural laws of physics listed above.

In order to provide a radiometrically valid sensor image, the rendering equation must include thermal self-radiation, reflected sunlight and sky, ambient radiation and atmospheric effects. The signature is affected by the optical properties of the object itself, but also by those of the surrounding objects. The atmosphere significantly affects the signature by attenuating the flux from the object and adding path radiance to the flux. Combining all these components ensures accuracy over the whole spectral range of operation; where reflected sun radiance dominates in the shorter wavelength regions and emitted radiance is more prominent in the longer wavelength bands. All calculations must be spectral calculations to account for the spectral nature of some sources (e.g. carbon dioxide (CO_2) in exhaust plumes) and spectral atmospheric transmittance. The main contributors to the optical signature are shown in Figure 4 (see[14] for a detailed description).

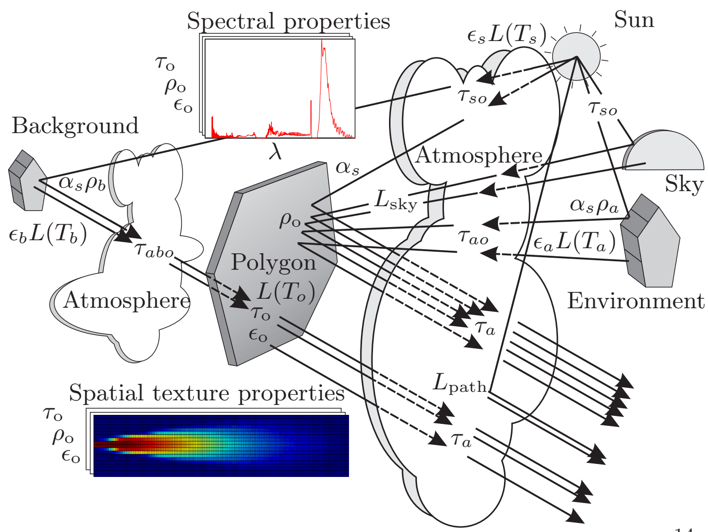

Figure 4: Main contributors to the radiometric signature.[14]

The *missile airframe* is the 'vehicle' of the seeker in the world. An accurate model of the airframe *flight behaviour* is required to steer the missile towards the target, using the seeker-provided target sight-line for missile *guidance*.These requirements are satisfied by detailed models for aerodynamics, flight control servos, the auto-pilot and guidance and navigation algorithms. The **natural laws of physics** in the areas of (1) temporal behaviour, (2) 6-dof kinematics, (3) aerodynamics, (4) mechanical behaviour and (5) control systems must be used in these models.

The *missile seeker* requires implementation of three main elements: (1) the sensor hardware system which provides the image, (2) the image processor that analyses the image for target detection and tracking, and (3) the gimballed platform which provides the signal for missile guidance.

The sensor hardware architecture provides the spatial definition for the **image renderer**. The simulated seeker images must be rendered in the specified spectral wavelength bands, with the required spatial resolution, using floating point calculations and including anti-aliasing techniques. Multi-colour images (e.g. for two-colour missile seekers) must be accurately registered as per the real world sensor.

The **sensor modelling** must reflect the characteristics of the real hardware seeker sensor. The modelling of various sensor types, e.g. reticle scanners, scanning detectors, or staring array sensors, must be supported. In this model, the detector defines the geometry of the image, as well as the multi-colour spectral domains. The field of view defines the extent of the observation in the world. The image quality affects the shape and temporal features of the image blobs and requires careful modelling of sensor optics (e.g. vignetting, point spread function), dome heating, detector properties (e.g. non-uniformities), detector and electronic noise, scanning mechanism effects and temporal temperature effects. An electronics signal transfer function processing capability is required to provide calibrated gray scale images as per the real hardware. Time delays in the system need to be modelled to account for any temporal effects which can affect target tracking.

An *image processing algorithm* development environment is required to support the optimisation of image processing, target tracking and missile guidance algorithms. The image processor algorithms require accurate images to support the calculation of dynamic, temporal, shape and colour blob features, used for target detection and tracking, as well as countermeasure rejection.

The *seeker gimballed platform* stabilises the sensor sightline against missile vibration and base motion. The *tracking* system responds to the image processing algorithms and aims to keep the target being tracked in the centre of the sensor field of view and provides the target sight-line rate as input to the missile guidance system. Simulation of the mechanical gimbal, inertial and angular sensors, stabilisation and control systems, according to the **natural laws of physics** require accurate modelling in the areas of (1) temporal behaviour, (2) 6-dof kinematics, (3) mechanical behaviour and (4) control systems.

The wider scope of the engagement requires a **simulation infrastructure** that supports modelling of a virtual three-dimensional world containing all the elements of the real world scenario. The simulation must provide the support infrastructure that will enable the missile seeker developer or countermeasure specialist developer to focus on their specific task at hand, rather than the natural laws of physics.

5. IMAGING SIMULATION SYSTEM

The Optronic System Simulator[15–17] (OSSIM) is a physics-based scene simulator that creates synthetic images of arbitrarily complex scenes in the visual and IR bands, covering the 0.4–14 μm spectral region. Various aircraft, missiles and other airborne, sea-based and ground-bound objects and countermeasures are viewed against clear sky, overcast sky and terrain and sea clutter backgrounds.

The system creates radiometrically accurate images simultaneously in multiple spectral bands, implementing physics equations, using in-band spectral radiometry and floating point image rendering. In order to provide correct colour ratios, the target and background signature radiance includes self-emitted flux, reflected sunlight, ambient radiance and sky radiance. Accurate surface temperature behaviour is modelled, either by aerodynamic heating or solar (thermodynamic) heating. A high fidelity three-dimensional complex hull geometrical model and temporally variable spatial texture modelling provide the shape and texture detail variation of targets, countermeasures and backgrounds. Partial transparency allows for accurate representation of gas clouds, countermeasure flares and aircraft plumes. The full scope of MODTRAN[18] atmospheric modelling, including spectral attenuation and path radiance, are available by embedding the MODTRAN computer code. Dynamics and kinematic behaviour of all objects in the world are modelled in six degrees of freedom. An advanced library provides support for control systems modelling.

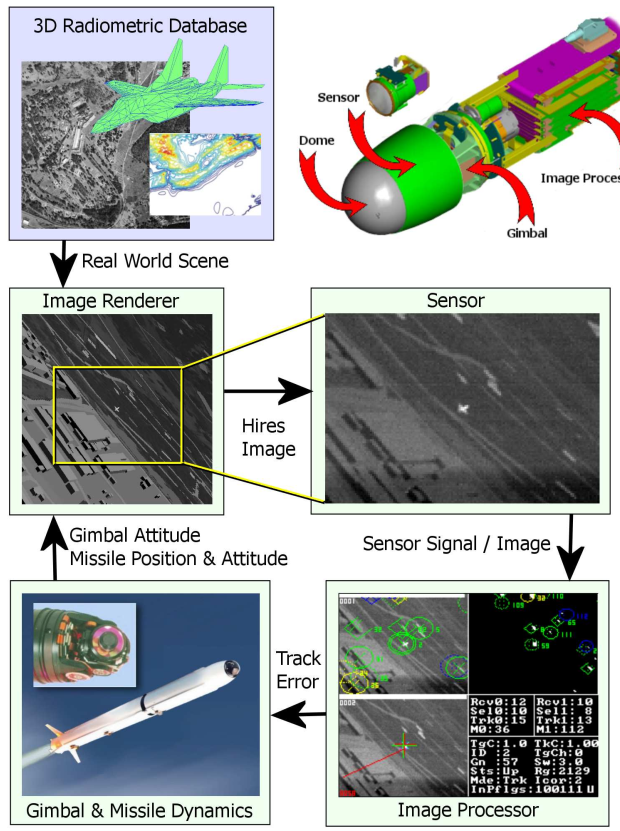

Figure 5: Imaging infrared missile closed loop simulation model components in OSSIM.

Models of the applicable weapon sub-systems mimic the real-world hardware operation; including functionality, performance and degradation effects. The elements of a scenario are described in the three-dimensional virtual world database that contains dynamic and/or static targets, countermeasures, terrain and various background objects, including realistic atmospheric conditions. The image renderer extracts the three-dimensional scene data from the database and renders 'ideal' two-dimensional images. These images are computed at a higher resolution than the weapon system camera resolution, for subsequent sensor image calculation to a lower resolution. For an imaging IR missile application (Figure 5), the sub-system models describe the various missile sub-systems: the sensor sub-assembly, the image processing, the mechanical gimbal, as well as the missile dynamics and kinematics (guidance, aerodynamics and flight).

The primary use for OSSIM includes development, optimisation and performance prediction in the areas of (1) missile seeker sensors and thermal imager systems, (2) signal and image processing algorithms, (3) sensor algorithms, (4) missile seeker countermeasures, and (5) aircraft self-protection against missile attacks.

6. KEY REQUIREMENTS ANALYSIS

OSSIM was used to analyse a selection of the key requirements listed in Figure 3. In some instances the requirement for the need is demonstrated and in other cases the requirements are quantified. The detail requirements for modelling of control systems and mechanical motion are beyond the scope of this paper, but the need for such modelling has been identified.

6.1 Image rendering

It is shown in Section 3.1 that an object's shape in the image (or as masked by the reticle) is an important discrimination feature. The provision of realistic simulated images, as seen by the missile seeker, is therefore a critical requirement.

In rendering an image, radiance from three-dimensional shapes in object space is rendered or mapped into two-dimensional irradiance shapes in the image plane. The radiometric rendering equation[14] is used to determine the irradiance distribution in the focal plane. Image rasterisation is the next step: calculating, from the irradiance distribution in the focal plane, the discrete pixel values in the image. When rasterising lines, the image pixel coordinate calculation during rasterisation can be done in integer arithmetic or floating point arithmetic.

Real world objects have continuous, smooth curves and lines in the image plane. Images however, have a discrete number of pixels available to represent the image of the smooth real world. Individual pixels in an image, normally of the same shape and size, can hold only single scalar values. By default, the pixel value is calculated at the centre of the pixel, and not as an average over the full area of the pixel. This spatial image discretisation results in jagged edges and lines, known as aliasing. The jagged line aliasing effect is also present in IR image rendering. However, a bigger challenge is to accurately render radiometric images for objects at long ranges, i.e. sub-pixel targets. A target at long distance fills only a fraction of the pixel, yet the pixel can have only one scalar value.

The technique of super-sampling is one way to improve on image quality with respect to radiometric accuracy as well as minimising jagged lines. In super-sampling, regions of the image are rendered at higher resolution than is required in the final image. As opposed to a single calculated pixel value in the pixel centre, the pixel (or small region) is expanded a few hundred times, filled with the appropriate pixel values as background. The target is then rendered in fine detail in the expanded image, to get a much more accurate radiometric value when down-sampling again, back to the original image. The result is an accurate radiometric image with less jagged edges and accurate estimations of pixels containing small targets. The number of samples in the super-sampling process determines the quality of the output—typical super-resolution image sizes are 256 to 512 pixels.

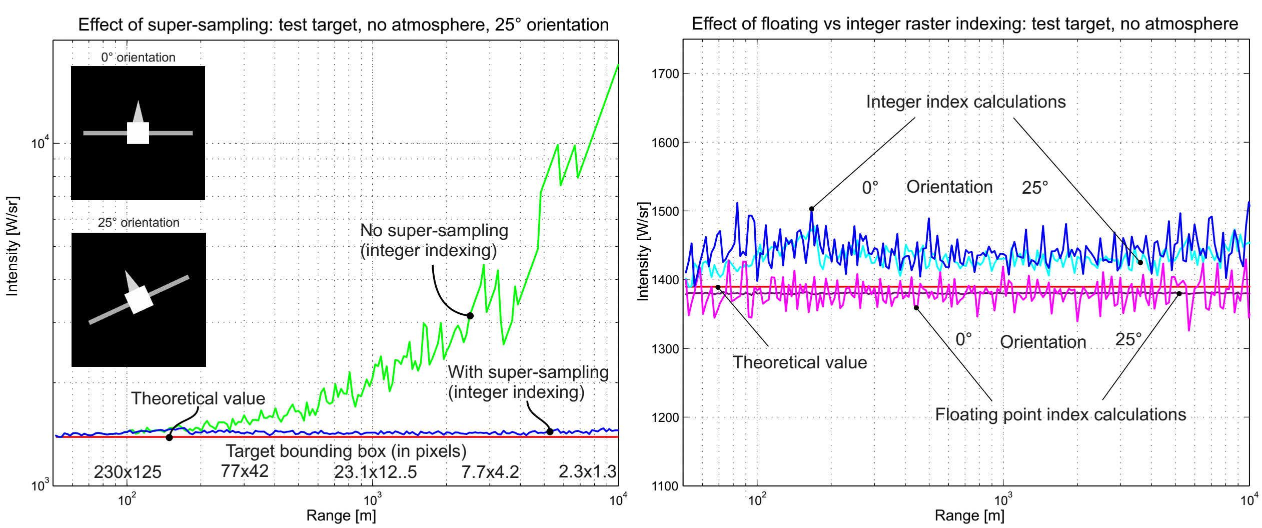

(a) Effect of super-sampling.

(b) Comparing float and integer render indexing.

Figure 6: Super-sampling and rendering index calculation for target ranges from 50 to 10 000 m.

A simple frontal aspect aircraft-shaped test target, comprising a square and triangles, was used in a simulation study on super-sampling. The theoretical value of the intensity was manually calculated in a unity spectral band from 8 to 12 μm. Simulated images with resolution of 512×512 were calculated, for target ranges from 50 m to 10 000 m, omitting the effect of the atmosphere. Figure 6a shows the calculated target intensity in the instances where super-sampling was either omitted or included in image rendering, versus the theoretical baseline.

Figure 6a shows an increasing intensity error for increasing range, with no super-sampling when calculated with an integer index rasteriser. It is evident that super-sampling is essential when the area of the bounding box around the target is less than 77×42=3234 pixels in size. This is a rather startling observation! Not shown here, is the observation that for a *floating point* index rasteriser, with no super-sampling, the intensity calculations *decrease* with increase in distance, disappearing completely at the relatively close range of 4.7 km (one to two pixels on target).

The effect of the choice of a rasteriser on intensity is shown in Figure 6b. The integer and floating point rasterisers were used to calculate the test target intensity in orientations of 0° and 25°. Both cases were done with super-sampling. From the intensity graph it is evident that the rasteriser using integer index calculations overestimates the target intensity. The integer rasteriser is not very sensitive to the orientation of polygon edges in the image, but has significant variation in target intensity depending on the pixel coverage on the target. The floating point Hecker rasteriser[19] results in a slight underestimation of target intensity. It is interesting to note that the floating point rasteriser favours slanted polygon edges—the 25° oriented target has almost no variation, compared to the 0° oriented target.

6.2 Temporal signatures

On the assumption that an object's signature can be lumped into a single area of uniform radiance, it can be shown[20] that the temporal intensity signature of an object is given by

$$I(t) = A(t) \int \epsilon L(T(t)) \mathcal{S} \tau_a d\lambda, \quad (1)$$

where $I(t)$ is the intensity as function of time, $A(t)$ is the area as function of time, ϵ is the spectral emissivity (assumed temporally constant), $L(T(t))$ is the Planck Law spectral radiance for an object at temperature T as function of time, $\mathcal{S}$ is the sensor spectral response and τ_a is the atmospheric spectral transmittance. This model is not very sophisticated, but sufficient for first-order modelling of objects with highly concentrated radiance, such as countermeasure flares and aircraft tailpipes.

Countermeasure flare signatures are typically highly variable; both between samples and in a temporal sense. Figure 7 shows a (normalised) model of temporal values for temperature, area and intensity, for the 1.8–2.6 μm (SWIR) and 3.6–4.8 μm (MWIR) spectral bands. This model accurately represents fairly typical measured values. Also shown is the intensity colour ratio, defined as SWIR/MWIR. The intensity values shown here corresponds with measured intensity values (SWIR intensity values scaled up for security requirements), while the temperature and area values represent values determined from analysis of the measured spectral emissivity, intensity and number of pixels in the images. The behaviour depicted here is not generic across all spectrally matched flares, but this particular case is critically important from a missile countermeasure perspective.

Close inspection of the first few hundred milliseconds' values indicates a sharper rise in intensity and apparent temperature in the SWIR band, compared to the MWIR band. The apparent areas' risetimes are similar. The difference in temperature/intensity rise-time results in a significant colour ratio peak, significantly beyond the stationary value. This colour ratio peak in the initial phase will greatly affect the missile's countermeasure response, and hence the seeker's classification of the flare—in this case, as a countermeasure flare to be rejected. The lower colour ratio later in the burn time is of no value. Please note that the important message here is the initial colour ratio peak shape (true to measured data) and not the absolute colour ratio (adjusted for security release requirements).

From Equation 1 and Figure 7 it is evident that the simulation must be able to accurately model the temporal values of emissivity, area and temperature to obtain the correct intensity. The requirement to obtain correct values of intensity *and* colour ratio, requires that *the combination* of temporal temperature and temporal area

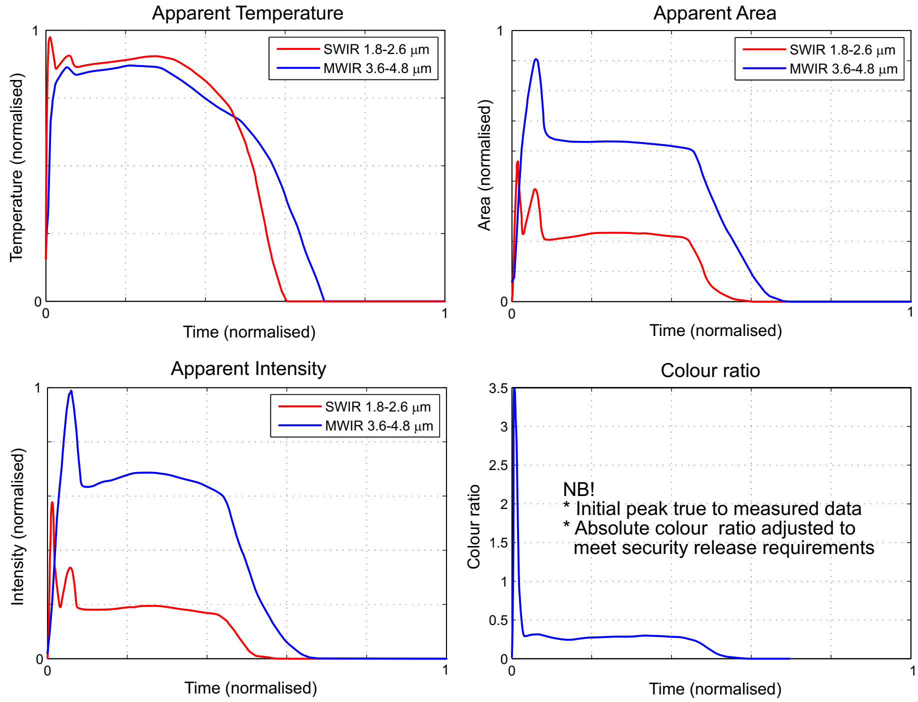

Figure 7: Temporal signature of countermeasure flare.

be correct. Furthermore, the temporal values must be modelled at very short time intervals, in order to capture fast transient events.

6.3 Solar reflection, sky background and the spectral colour ratio

Solar reflection plays an important role in optical signatures of cooler objects at wavelengths shorter than 3 μm, and sometimes even in the 3–5 μm spectral band. Likewise does the sky background (clear sky, or especially clouds) affect the contrast-based signatures in the shorter wavelengths. The colour ratio of hot objects, such as countermeasure flares is less affected by solar reflection. The colour ratio of cooler objects is important, since it may affect the countermeasure operation of two-colour missiles.

Figure 8 shows some results obtained, using the OSSIM simulation, for a small fighter aircraft, at idle engine setting (neglible plume contribution). Time of day was early in the morning, with the sun just above the horizon, to emphasise the sun-lit and shady views of the aircraft. The clear sky background was calculated using MODTRAN's path radiance to space, along the view direction. The radiometric signature comprised self-emittance, reflected ambient light, atmospheric path radiance, and reflected sunlight. The sun is located at 90° with respect to the aircraft forward direction; 0–180° is the sunlit side and 180–360° is the shade side. Aircraft range is 1 km. The atmosphere is a Mid-latitude summer, altitude 100 m. Note, in the plots, a jagged variation in intensity: this is a result of rendering a polygon model in a raster image.

In Figure 8 we consider the colour ratio as the 1.8–2.5 μm intensity divided by the 3–5 μm intensity (for the absolute and contrast cases). The arithmetic ratio is but one colour measure, several other measures can also be devised. Indeed, the concept of true arithmetic colour ratio is undefined for contrast signatures, since the contrast signature depends on the background radiance.

It is evident in Figure 8 that the 3–5 μm signature is not significantly affected by the presence of sun irradiance. The signature in the 1.8–2.5 μm spectral band is strongly affected by reflected sunlight. The effect of the sun on the colour ratio is significant. The absolute value of the contrast colour ratio can be as large as one; which could affect the countermeasure processing in some missiles.

The presence of atmospheric path radiance significantly affects the contrast signature of cooler objects. Path radiance is the primary component of clear sky background radiance.

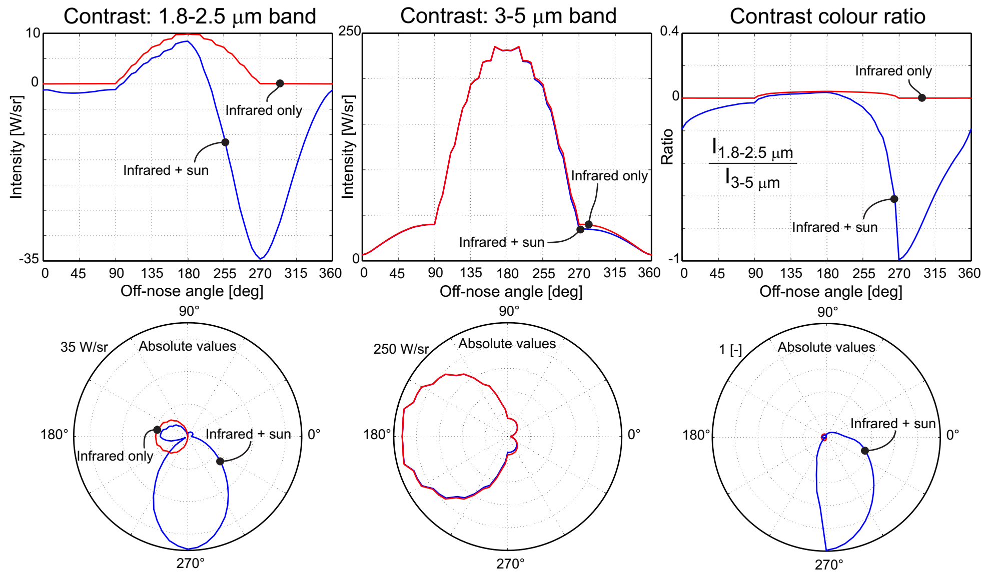

(a) Contrast (against clear sky) intensity and colour.

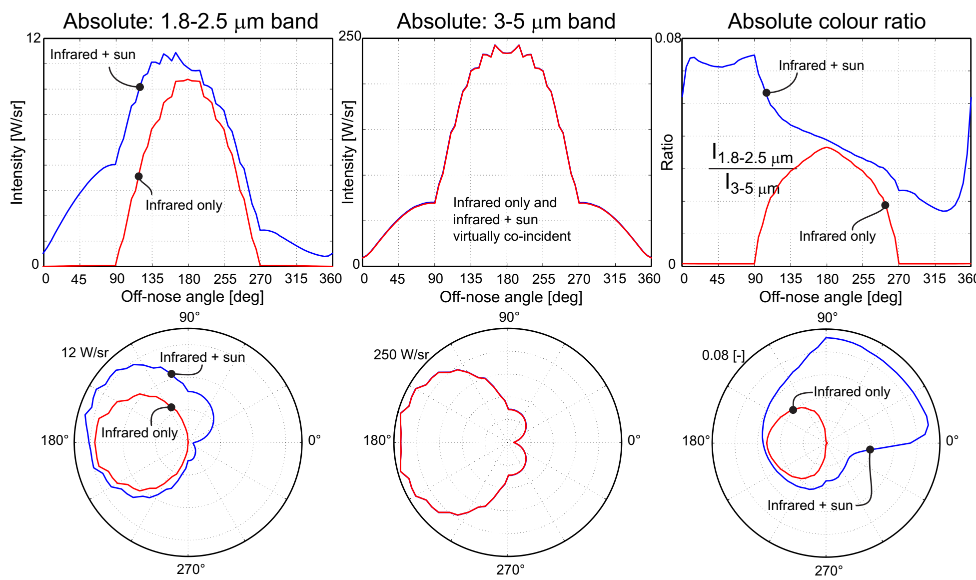

(b) Absolute intensity and colour.

Figure 8: Aircraft fuselage (idle engine setting) intensity colour ratio: 1.8–2.5 μm to 3–5 μm.

Figure 9 shows the colour of an MTV flare, a spectrally matched flare, an aircraft with plume, clear sky and cloud. In this case the colour ratio is defined as the pixel irradiance in 3–5 μm divided by pixel irradiance in 1.8–2.5 μm. Transmittance and path radiance were calculated with the Modtran Tropical atmospheric model. The cloud signature in the shorter wavelengths is mainly caused by reflected sunlight. From this figure it is evident that a two-colour ratio can be used quite effectively to classify and suppress sunlit cloud backgrounds.

From the information in this section it is evident that reflected sunlight and sky radiance are essential for accurate colour measure rendering. Colour measures can be complex in itself and require very careful consideration in image simulation systems.

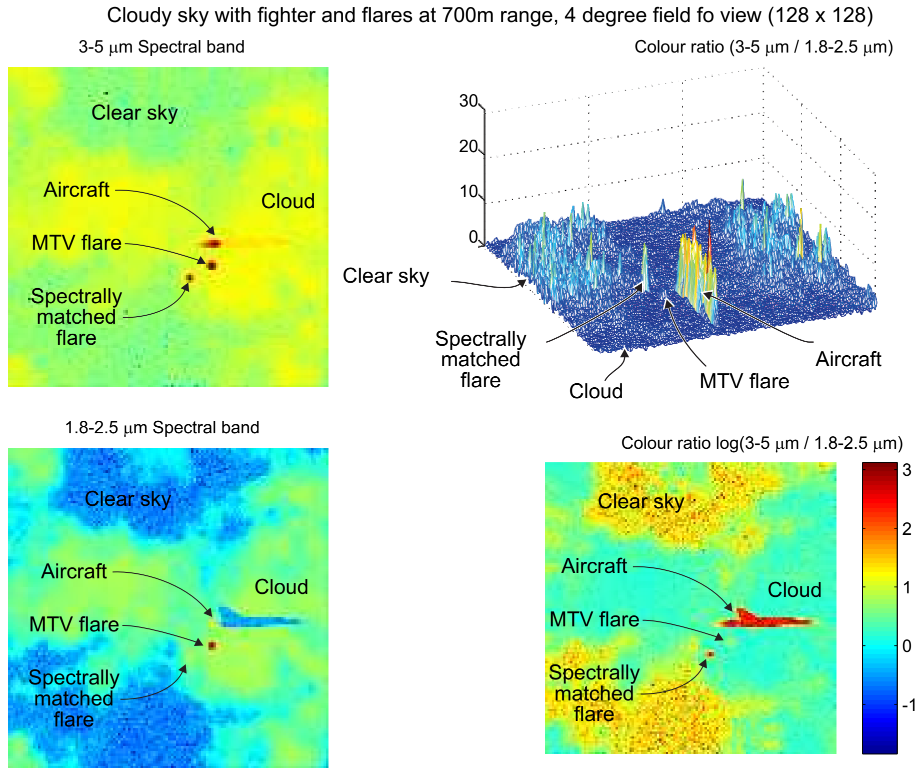

Figure 9: Countermeasure flares, cloud and aircraft fuselage intensity colour ratio: 3–5 μm to 1.8–2.5 μm.

6.4 Spectral atmospheric properties and target signature

The effective transmittance, a scalar approximation of the spectral transmittance, is defined by[20]

$$\tau_a(R) = \frac{\int_0^\infty \epsilon_\lambda L_\lambda(T)\tau_{a\lambda}(R)\mathcal{S}_\lambda d\lambda}{\int_0^\infty \epsilon_\lambda L_\lambda(T)\mathcal{S}_\lambda d\lambda} \tag{2}$$

where ϵ_λ is the spectral emissivity, $L_\lambda(T)$ is the Planck Law spectral radiance for a source temperature T, $\mathcal{S}_\lambda$ is the sensor spectral response and $\tau_{a\lambda}(R)$ is the atmospheric spectral transmittance for distance R.

Spectral atmospheric transmittance values were calculated using MODTRAN,[21] for a number of distances. Equation 2 was used to determine the effective transmittance for several different thermal sources as a function of range. These sources included hot grey body radiators at temperatures ranging from 330 K to 2300 K, as well as spectrally selective radiation from hot CO_2 emission from an aircraft plume. The sensor response shown in Figure 10a was used. The effective transmittance values so determined are shown in Figure 10b. Note the severe attenuation for the plume signal, even over short ranges. This stems from the fact that the plume spectral emittance is caused by the hot CO_2 in the plume, but is also attenuated by the cold CO_2 in the atmosphere. This observation is relevant to the flux transfer from narrow spectral radiators (such as gas molecules), through a medium with spectral selective attenuation.

It is often proposed that the effective transmittance versus distance can be approximated by an exponential curve, $\tau_a = e^{-\alpha R}$, Bouguer's Law at a single wavelength. This approximation is not always acceptable, as is clearly evident in Figure 10b. A visual best-fit exponential to the graphs yielded an attenuation coefficient $\alpha = 0.3$ km^{-1}. It is a poor fit for all the cases considered. It is therefore essential that accurate spectral calculations be performed to account for the CO_2 absorption in the 3–5 μm band, not only for spectrally selective sources, but also for grey body sources.

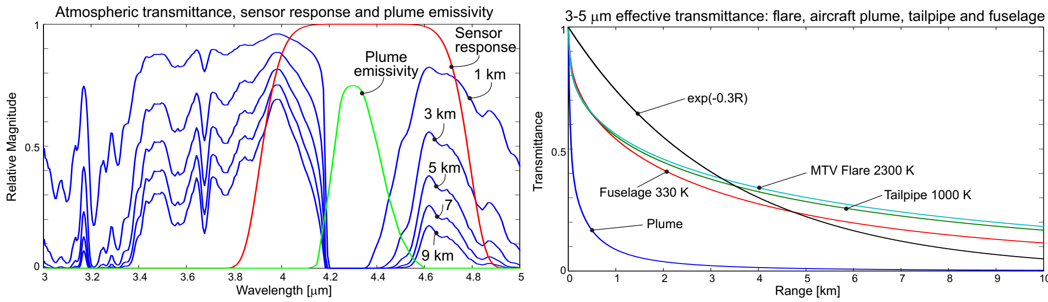

(a) Spectral atmospheric transmittance for a range of altitudes, plume emissivity and sensor response.

(b) Effective transmittance for plume, fuselage, tailpipe and flare, and Bouguer's Law transmittance approximation.

Figure 10: Investigation into the effect of spectral transmittance on effective transmittance calculation.

6.5 Flight dynamics and kinematics behaviour

It is stated in Section 3.2 that the (relative) movement of objects in the scene is an important countermeasure feature.

Missiles and aircraft exhibit very complex flight dynamics and internal kinematics (e.g. inertial sensors, gimbal systems and servos). The kinematics are normally controlled by sophisticated control systems for gimbal control, tracking and guidance and flight surface control. Domain experts normally develop these simulation models.[22,23] Modelling flare dynamics require less sophistication, but the developer is still left with questions regarding the temporal mass decrease, and aerodynamics drag[24] and its temporal variation. Figure 11 shows a simple flare dynamics model that accounts for drag, airflow turbulence and the direction of the velocity vector.

The simulation must provide a library to support the accurate calculation of kinematic, aerodynamic, and guidance and control system behaviour.

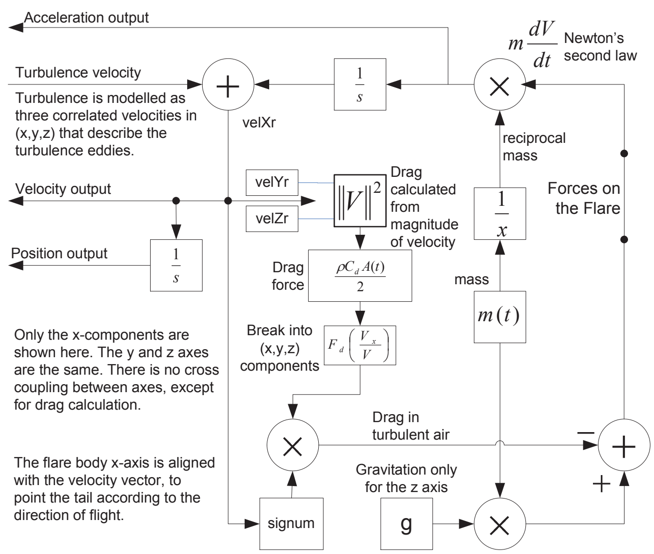

Figure 11: Flare kinematics model.

6.6 Missile seeker dome heating

The effect of the heated dome and heated, compressed air on the performance of an imaging sensor was studied in a closed loop supersonic missile flight simulation.[16] This type of analysis is very difficult, if not impossible, in a real world missile flight test. The dome temperature and its effect on the seeker performance was investigated for various mach numbers and ambient temperatures.

During supersonic missile flight, the air in front of the dome is heated and compressed to such an extent that the CO_2 in the air becomes a significant source of infrared radiation in the mid-IR. The CO_2 band radiation model developed by Bernstein[25] was used in the sensor model.

The top graph of Figure 12 shows the dome and compressed air temperature variation during the flight. The flux contribution of the dominant radiating sources is shown in the second graph.

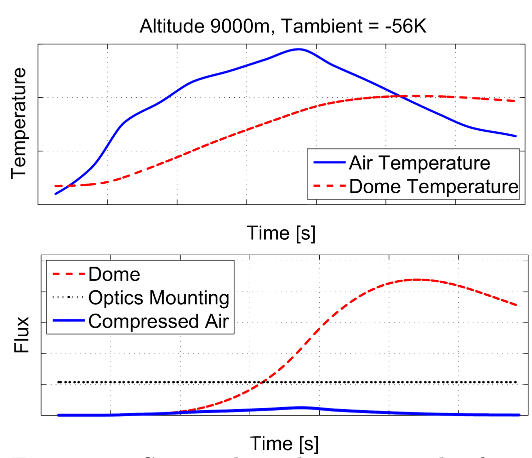

Figure 12: Sensor dome heating results for a simulated supersonic missile flight.

Initially, the radiation of the optics mounting is the main contributor, but as the dome temperature increases during flight, radiation from the dome becomes dominant. Note that although the temperature of the heated air is higher than that of the dome, the flux from the dome dominates due to the dome broadband emissivity exceeding the emissivity of the air.

The considerable influence of the hot dome and heated air on the sensor operation, and hence indirectly on the image processing, detection and tracking algorithms, demonstrated the need for detailed and in-depth sensor modelling in the development environment.

7. CONCLUSION

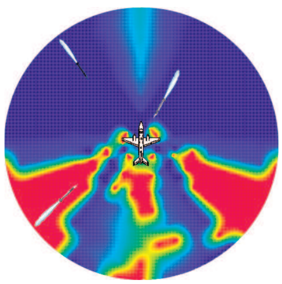

		Simulation key considerations																											
		Natural laws of physics														Image rendering					Sensor modelling								
		Radiometry					Atmosphere																						
		Spectral calculations	Thermal self-radiation	Reflected sunlight	Reflected sky radiance	Ambient radiation	Transmittance	Radiance	3D geometry & 2D texture	Thermal modelling	Temporal modelling	6-dof kinematics modelling	Aerodynamics modelling	Mechanical modelling	Control systems modelling	Anti-aliasing	Floating point calculations	Spatial resolution	Image registration	Multiple spectral bands	Optics	Dome heating	Detector properties	Detector & electronic noise	Scanning effects	Temporal temperature effects	Signal transfer function	Time delays	Simulation infrastructure
6.1	Image rendering															x	x	x	x	x									x
6.2	Temporal signatures	x	x						x	x	x																		x
6.3	Solar reflection, sky background and the spectral colour ratio	x	x	x	x	x																							x
6.4	Spectral atmospheric properties and target signature						x	x																					x
6.5	Flight dynamics and kinematics behaviour											x	x																x
6.6	Missile seeker dome heating														x						x	x	x	x	x	x	x	x	x

Figure 13: Key requirements analysis covered in this paper.

The paper showed that the missile aircraft engagement is a complex and sensitive system, which can easily be upset by small perturbations. The nature of the sophisticated target/countermeasure discrimination features used in modern missiles requires equally sophisticated simulation and modelling attention.

The analysis of the missile-aircraft engagement identified the key requirements for an infrared simulation system. OSSIM was used to evaluate a sub-set of these requirements (Figure 13). A more comprehensive coverage will require a fair sized book.

The investigation elevates some factors such as rendering aliasing errors, temporal signatures, in-band spectral calculations, reflected sunlight, path radiance, kinematics modelling and dome effects to the status of *primary requirements*. It is shown that these requirement must be met to accurately model and simulate the subtleties of the missile aircraft engagement.

The near-chaotic nature of the missile-aircraft engagement, with limited regions of marginally stable tracking (Figure 1), requires comprehensive modelling with careful attention to minute details, covering many specialist domains.

ACKNOWLEDGMENTS

The authors wish to thank Pieter Goede, Marlien Dreyer and Paul Retief for reviewing this paper.

REFERENCES

[1] Titterton, D. H., [*Mid-infrared Semiconductor Optoelectronics*], vol. 118/2006, ch. Development of Infrared Countermeasure Technology and Systems, 635–671, Springer Verlag (2006).

[2] Kopp, C., "Stealth in strike warfare," *Air Power International* **6**(1) (2000).

[3] Goddard, P., "Advanced infra red countermeasure solutions." Presented at the 2008 Association of Old Crrows (AOC) International Exhibition and Symposium at the Adelaide Convention Centre, Australia. http://www.oldcrows.org.au/files/2008(May 2008).

[4] Glasgow, B. and Bell, W., "The future of anti-aircraft imaging infrared seeker missile threats," in [*IEEE Aerospace Conference*], **3**, 457–465 (March 1999).

[5] Friedman, N., [*The Naval Institute Guide to World Naval Weapons Systems, 1997-1998*], Naval Institute Press (1997).

[6] Rafael Advanced Defense Systems, "Python-5, Full Sphere IR Ai-to-Air or Surface-to-Air Missile," Brochure Python-5/UNC/22801/0108/35/02 Graphic Design Dep/406, `www.rafael.co.il` (2012).

[7] Denel Dynamics, "A-Darter, Fifth-generation Air-to-Air Missile System," `http://www.deneldynamics.co.za/brochures/Broc0264_A-Darter%20External.pdf` (2012).

[8] Roger, S. K., Colombi, J., Martin, C., Gainey, J., Fielding, K., Burns, T., Ruck, D., Kabrisky, M., and Oxley, M., "Neural networks for automatic target recognition," *Neural Networks* **8(7/8)**, 1153–1184 (1995).

[9] Labonte, G. and Deck, W., "Infrared target-flare discrimination using a zisc hardware neural network," *Journal of Real-Time Image Processing* **5**(1), 11 – 32 (2010).

[10] Singstock, B. D., *Infrared Target Recognition*, Master's thesis, Electrical Engineering, Faculty of the School of Engineering of the Air Force Institute of Technology, Air University, Ohio (1991).

[11] Viau, C., "Expendable cm effectiveness against imaging ir-guided threats," in [*Second International Conference on Electronic Warfare-EWCI 2012, Bangalore, India*], (2012).

[12] S.Yu and Azimi-Sadjadi, M. R., "Neural network directed bayes decision rule for moving targe tclassification," in [*IEEE Transactions on Aerospace and Electronic Systems*], **36**, 176–188 (2000).

[13] Pictures. `http://www.randomclipart.com/14-cartoon-missile` and `http://www.hsgalleries.com/gallery04/mirage2000wp_1.htm` (2011).

[14] Willers, C. J. and Willers, M. S., "OSSIM: Optronics scene simulator white paper," Tech. Rep. 6700-PG-103400-01 Rev 3, Council for Scientific and Industrial Research (CSIR) (2011).

[15] Willers, C. J. and Wheeler, M. S., "Application of image simulation in weapon system development," in [*Proceedings: IX SIGE Electonic Warfare Conference*], (2007).

[16] Willers, M. S. and van den Bergh, J. S. H., "Optronics sensor development using an imaging simulation system," in [*Saudi International Electronics, Communications and Photonics Conference (SIECPC)*], IEEE Xplore (2011).

[17] Willers, C. J., Willers, M. S., and Lapierre, F. D., "Signature modelling and radiometric rendering equations in infrared scene simulation systems," in [*Technologies for Optical Countermeasures VIII*], Titterton, D. H. and Richardson, M. A., eds., **8187**, SPIE (2011).

[18] Berk, A., "Modtran 5.2.0.0 user's manual," tech. rep., Air Force Research Laboratory, Air Force Materiel Command, Hanscom AFB, Ma (2008).

[19] Hecker, C., "Perspective texture mapping part ii: Rasterization," *Game Developer* **95**, 18–26 (June/July 1995).

[20] Willers, C. J., [*Advanced Radiometry: Techniques for Real-World Applications*], SPIE Press (2013).

[21] MODTRAN, "MODTRAN atmospheric radiative transfer model." `http://www.modtran.org/` (2009).

[22] JSB-Sim (2010). `http://jsbsim.sourceforge.net/`.

[23] Thomson, D. and Bradley, R., "Inverse simulation as a tool for flight dynamics research - Principles and applications," *Progress in Aerospace Sciences* **42**(3), 174–210 (2006).

[24] Toothman, H. and Loughmiller, C., "F-4B and F-8 Flare Effectiveness Against the ATOLL Missile (AA-2)," NRL Memorandum Report 2297, Naval Research Laboratory (July 1971).

[25] Bernstein, L. S., "Band model parameters for the 4.3μm band from 200 to 3000k - II. prediction, comparison to experiment, and application to plume emission-absorption calculations," *Journal of Quantitative Spectroscopy and Radiative Transfer* **23**, 169–185 (May 1979).